

# Interpreting Transformer’s Attention Dynamic Memory and Visualizing the Semantic Information Flow of GPT

Shahar Katz

Yonatan Belinkov

Technion - Israel Institute of Technology

shachar.katz@cs.technion.ac.il

belinkov@technion.ac.il

## Abstract

Recent advances in interpretability suggest we can project weights and hidden states of transformer-based language models (LMs) to their vocabulary, a transformation that makes them human interpretable and enables us to assign semantics to what was seen only as numerical vectors. In this paper, we interpret LM attention heads and memory values, the vectors the models dynamically create and recall while processing a given input. By analyzing the tokens they represent through this projection, we identify patterns in the information flow inside the attention mechanism. Based on these discoveries, we create a tool to visualize a forward pass of Generative Pre-trained Transformers (GPTs) as an interactive flow graph, with nodes representing neurons or hidden states and edges representing the interactions between them. Our visualization simplifies huge amounts of data into easy-to-read plots that reflect why models output their results. We demonstrate the utility of our modeling by identifying the effect LM components have on the intermediate processing in the model before outputting a prediction. For instance, we discover that layer norms are used as semantic filters and find neurons that act as regularization vectors.

## 1 Introduction and Previous Work

*Wouldn't it be useful to have something similar to an X-ray for transformers language models?*

Recent work in interpretability found that hidden-states (HSs), intermediate activations in a neural network, can reflect the “thought” process of transformer language models by projecting them to the vocabulary space using the same transformation that is applied to the model’s final HS, a method known as the “logit lens” (nostalgebraist, 2020). For instance, the work of Geva et al. (2021, 2022b) shows how the fully-connected blocks of transformer LMs add information to the model’s residual stream, the backbone route of information,

promoting tokens that eventually make it to the final predictions. Subsequent work by Dar et al. (2022) shows that projections of activated neurons, the static weights of the models’ matrices, are correlated in their meaning to the projections of their block’s outputs. This line of work suggests we can stop reading vectors (HSs or neurons) as just numbers; rather, we can read them as words, to better understand what models “think” before making a prediction. These studies mostly interpret static components of the models or are limited to specific case studies that require resources or expertise.

To address the gap in accessibility to the mechanisms behind transformers, some studies create tools to examine how LMs operate, mostly by plotting tables of data on the most activated weights across generations or via plots that show the effect of the input or specific weights on a generation (Geva et al., 2022a; Hoover et al., 2020; Vig and Belinkov, 2019). Yet, such tools do not present the role of each of the LM’s components to get the full picture of the process.

In this paper, we interpret another type of weights of LMs via the logit lens: the attention module’s dynamic memory Vaswani et al. (2017). We describe the semantic information flow inside the attention module, from input through keys and values to attention output, discovering patterns by which notions are passed between the LM’s components into its final prediction.

Based on our discoveries, we model GPTs as flow-graphs and create a dynamic tool showing the information flow in these models (for example, Figure 1). The graph makes it easy to detect the effect on the prediction of single to small sets of neurons during forward passes. We use this tool to analyze GPT-2 (Radford et al., 2019) in three case studies: (1) we reflect the mechanistic analysis of Wang et al. (2022) on indirect object identification in a simple way; (2) we analyze the role of layer norm layers, finding they act as semantic filters;

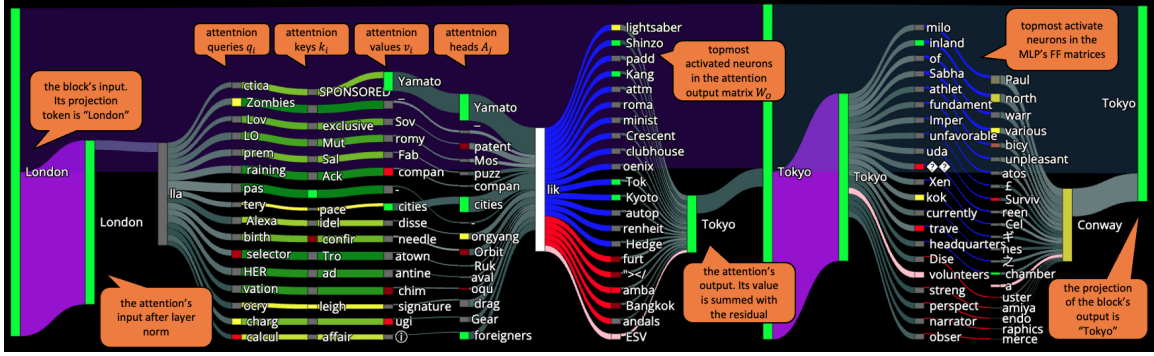


Figure 1: Modeling a single layer of GPT-2 for the prompt: “The capital of Japan is the city of”. Each node represents a small group of neurons or HS, which are labeled by the top token of their projection to the vocabulary space. The plot should be read from left to right and includes the attention block: LN (the node at the end of the first purple edge), query, memory keys and values (with greenish edges) and the topmost activated attention output neurons (in blue and red), followed by the MLP: LN (in purple), first and second matrices’ most activated neurons (in blue and red). The dark edges in the upper parts of the plot are the residuals of each sub-block.

and (3) we discover neurons that are always activated, related to but distinct from rogue dimensions (Timkey and van Schijndel, 2021), which we term regularization neurons.

We share our code and tool for public use.<sup>1</sup>

## 2 Background

### 2.1 The Transformer Architecture

We briefly describe the computation in an autoregressive transformer LM, such as GPT-2, and refer to Vaswani et al. (2017) and Elhage et al. (2021) for more information.<sup>23</sup>

The model consists of a chain of blocks (layers), that read from and write to the same residual stream. The input to the model is a sequence of word embeddings,  $x_1, \dots, x_t$  (the length of the input is  $t$  tokens), and the residual stream propagates them into deeper layers, referring to the intermediate value it holds at layer  $l$  while processing the  $i$ -th token as  $hs_i^l$  ( $hs_i$  in short). The HS at the final token and top layer,  $hs_t^L$ , is passed through a layer norm,  $ln_f$ , followed by a decoding matrix  $D$  that projects it to a vector the size of the vocabulary. The next token probability distribution is obtained by applying a softmax to this vector.

Each block is made of an attention sub-block (module) followed by a multi-layer perceptron (MLP), which we describe next.<sup>4</sup>

<sup>1</sup><https://github.com/shacharkZ/Visualizing-the-Information-Flow-of-GPT>.

<sup>2</sup>Appendix A details these models in the context of our graph modeling.

<sup>3</sup>For simplicity we do not mention dropout layers and position embeddings here.

<sup>4</sup>In models such as GPT-J (Wang and Komatsuzaki, 2021),

### 2.2 GPTs Sub-Blocks

**Attention:** The attention module consists of four matrices,  $W_Q, W_K, W_V, W_O \in \mathbb{R}^{d \times d}$ . Given a sequence of HS inputs,  $hs_1, \dots, hs_t$ , it first creates three HS for each  $hs_i$ :  $q_i = hs_i W_Q$ ,  $k_i = hs_i W_K$ ,  $v_i = hs_i W_V$ , referred to as the current queries, keys, and values respectively. When processing the  $t$ -th input, this module stacks the previous  $k_i$ ’s and  $v_i$ ’s into matrices  $K, V \in \mathbb{R}^{d \times t}$ , and calculates the attention score using its current query  $q = q_t$ :  $A = \text{Attention}(q, K, V) = \text{softmax}\left(\frac{qK^T}{\sqrt{d}}\right)V$ . In practice, this process is done after each of  $q_i, k_i, v_i$  is split into  $h$  equal vectors to run this process in parallel  $h$  times (changing the dimension from  $d$  to  $d/h$ ) and to produce  $A_j \in \mathbb{R}^{\frac{d}{h}}$  ( $0 \leq j < h$ ), called heads. To reconstruct an output in the size of the embedding space,  $d$ , these vectors are concatenated together and projected by the output matrix:  $\text{Concat}(A_0, \dots, A_{h-1})W_O$ . We refer to the process of this sub-block as  $\text{Attn}(hs)$

We emphasize that this module represents dynamic memory: it recalls the previous values  $v_i$  (which are temporary representations for previous inputs it saw) and adds a weighted sum of them according to scores it calculates from the multiplication of the current query  $q_t$  with each of the previous keys  $k_i$ .

**MLP:** This module consists of an activation function  $f$  and two fully connected matrices,  $FF_1, FF_2^T \in \mathbb{R}^{d \times N}$  ( $N$  is a hidden dimension, usually several times greater than  $d$ ). Its output is

the two sub-blocks work in parallel. In this work we focus on GPT-2’s sequential architecture.

$$MLP(x) = f(xFF_1)FF_2.$$

**Entire block:** GPT-2 applies layer norm (LN), before each sub-block:  $ln_1$  for the attention and  $ln_2$  for the MLP. While LN is thought to improve numeric stability (Ba et al., 2016), one of our discoveries is the semantic role it plays in the model (subsection 5.2). The output of the transformer block at layer  $l$ , given the input  $hs_i^l$ , is

$$hs_i^{l+1} = hs_i^l + \text{Attn}(ln_1(hs_i^l)) + MLP(ln_2(\text{Attn}(ln_1(hs_i^l)) + (hs_i^l))) \quad (1)$$

### 2.3 Projecting Hidden States and Neurons

**The Logit Lens (LL):** nostalgebraist (2020) observed that, since the decoding matrix in GPTs is tied to the embedding matrix,  $D = E^T$ , we can examine HS from the model throughout its computation. Explicitly, any vector  $x \in \mathbb{R}^d$  can be interpreted as a probability on the model’s vocabulary by projecting it using the decoding matrix with its attached LN:

$$LL(x) = \text{softmax}(ln_f(x)D) = s \in \mathbb{R}^{|vocabulary|} \quad (2)$$

By applying the logit lens to HS between blocks, we can analyze the immediate predictions held by the model at each layer. This allows us to observe the incremental construction of the model’s final prediction, which Geva et al. (2022b) explored for the MLP layers.

Very recent studies try to improve the logit lens method with additional learned transformations (Belrose et al., 2023; Din et al., 2023). However, we stick with the basic approach of logit lens since we wish to explore the interim hypotheses formed by the model, rather than better match the final layer’s output or shortcut the model’s computation.

**Interpreting Static Neurons:** Each of the mentioned matrices in the transformer model shares one dimension (at least) with the size of the embedding space  $d$ , meaning we can disassemble them into neurons, vectors that correspond to the “rows” or “columns” of weights that are multiplied with the input vector, and interpret them as we do to HS. Geva et al. (2021) did this with single neurons in the MLP matrices and Dar et al. (2022) did this with the interaction of two matrices in the attention block,  $W_Q$  with  $W_K$  and  $W_V$  with  $W_O$ , known as the transformer circuits  $QK$  and  $OV$  (Elhage et al., 2021). These studies claim that activating a neuron whose projection to the vocabulary has a specific

meaning (the common notion of its most probable tokens) is associated with adding its meaning to the model’s intermediate processing.

In our work we interpret single and small groups of HS using the logit lens, specifying when we are using an interaction circuit to do so. In addition, while previous studies interpret static weights or solely the attention output, we focus on the HS that the attention memory recalls dynamically.

### 3 Tracing the Semantics Behind the Attention’s Output

In this section, we trace the components which create the semantics of the attention block’s output, by comparing vectors at different places along the computation graph. In all the following experiments, we project HS into the vocabulary using the logit lens to get a ranking of all the tokens, then pick the top- $k$  tokens according to their ranking. We measure the common top tokens of two vectors ( $v_1$  and  $v_2$ ) via their intersection score  $I_k$  (Dar et al., 2022):

$$I_k(v_1, v_2) = \frac{LL(v_1)[\text{top-k}] \cap LL(v_2)[\text{top-k}]}{k} \quad (3)$$

We say that two vectors are semantically aligned if their  $I_k$  is relatively high (close to 1) since it means that a large portion of their most probable projected tokens is the same.

Throughout this section, we used CounterFact (Meng et al., 2022), a dataset that contains factual statements, such as the prompt “*The capital of Norway is*” and the correct answer “*Oslo*”. We generate 100 prompts randomly selected from CounterFact using GPT-2-medium, which we verify the model answers correctly. We collect the HSs from the model’s last forward-passes (the passes that plot the answers) and calculate  $I_{k=50}$ .<sup>5</sup>

#### 3.1 Projecting the Attention Memory

For our analysis we interpret  $W_V$  products, the attention’s heads  $A_j$  and its memory values,  $v_{ji}$  ( $j$  for head index and  $i$  for token index). For each component we calculate its mean  $I_{k=50}$  with its attention block output ( $\text{Attn}(hs_i^l)$ , “ $I_k$  attn”), its transformer block output ( $hs_i^{l+1}$ , “ $I_k$  block”), and the model’s final output ( $hs_i^L$ , “ $I_k$  final”).

Dar et al. (2022) suggest using the  $OV$  circuit, in accordance to Elhage et al. (2021), to project

<sup>5</sup>Refer to Appendix B, C.1 for more information about our model selection and setup.

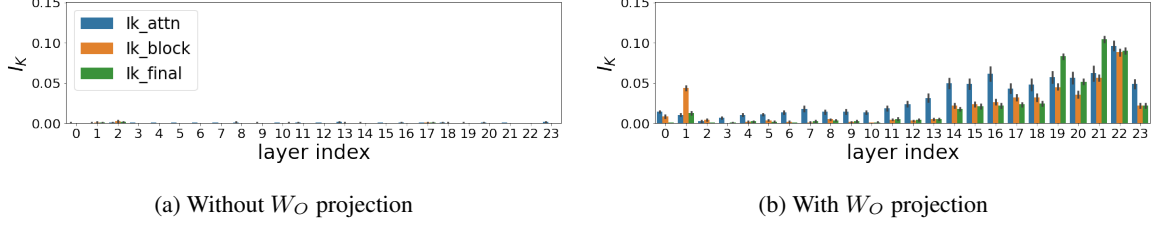
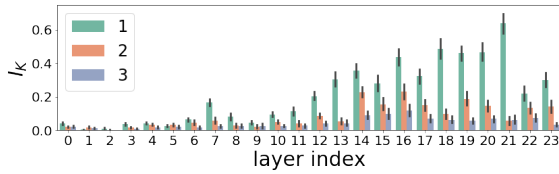


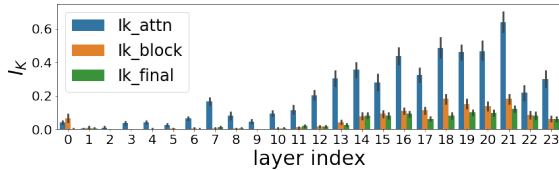
Figure 2: Comparing  $I_{k=50}$  token projection alignment between the mean of all heads  $A_j$  with different parts of the model's, with and without using the attention block's  $W_O$  matrix for projection, suggesting that the output of the attention block's  $W_V$  operates in a different space and that  $W_O$ 's role is to adjust it to the common embedded space.

the neurons of  $W_V$  by multiplying them with  $W_O$ . Similarly, we apply logit lens to  $A_j$  once directly and once with the  $OV$  circuit, by first multiplying each  $A_j$  with the corresponding parts of  $W_O$  to the  $j$ -th head ( $j : j + \frac{d}{h}$ ). While the first approach shows no correlation with any of the  $I_k$  we calculate (Figure 2a), the projection with  $OV$  shows semantic alignment that increase with deeper layers, having some drop at the final ones (Figure 2b). The pattern of the latter is aligned with previous studies that examine similar scores with the MLP and the entire transformer block (Haviv et al., 2023; Lamparth and Reuel, 2023; Geva et al., 2022b), showing that through the  $OV$  circuit there is indeed a semantic alignment between the attention heads and the model's outputs and immediate predictions.

This finding suggests that the HS between  $W_V$  and  $W_O$  do not operate in the same embedded space, but are rather used as coefficients of the neurons of  $W_O$ . Therefore, outputs of  $W_V$  should be projected with logit lens only after they are multiplied by  $W_O$ .



(a) Mean  $I_{k=50}$  for only the top 3 heads with the largest norm, comparing to attention block output.



(b) Mean  $I_{k=50}$  for only the head with the largest norm, comparing to attention block output, layer output and the model's final output.

Figure 3: Projecting attention heads

### 3.2 Projecting Only the Top Attention Heads

The effect of each head is not equal since each has a different norm, sometimes making a few more dominant than others when they are concatenated together into one vector. We separately ranked each attention block's heads with the  $OV$  circuit ( $A_j W_O$ ) according to their norms and repeated the comparison. We found that only the few heads with the largest norm have a common vocabulary with their attention block output (Figure 3a), which gradually increases the effect on the blocks' outputs and the final prediction (Figure 3b). This suggests that the attention block operates as a selective association gate: by making some of the heads much more dominant than others, this gate chooses which heads' semantics to promote into the residual (and which to suppress).

### 3.3 Projecting Memory Values

We ran the same experiment comparing the memory values  $v_{ji}$ , the values that the attention mechanism recalls from the previous tokens. For each head  $A_j$ , we rank its memory values based on their attention scores and observe that memory values assigned higher attention scores also exhibit a greater degree of semantic similarity with their corresponding head. The results for the top three memory values are illustrated in Figure 4.

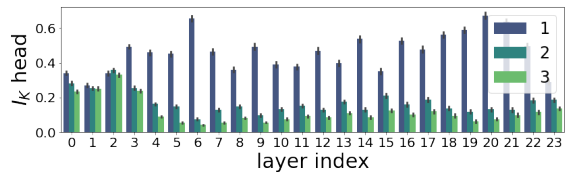


Figure 4: Mean  $I_{k=50}$  for the 3 top biggest by attention score memory values, comparing to their head output.



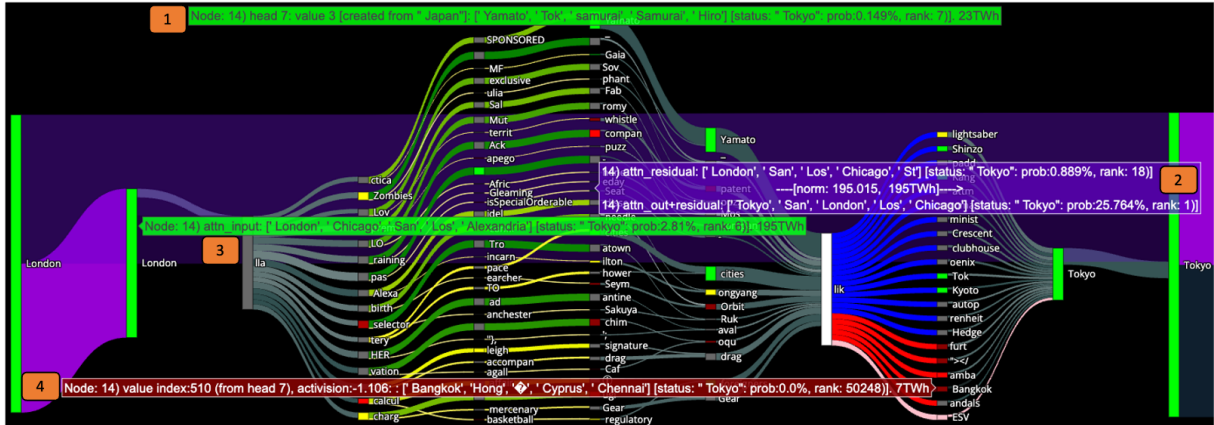


Figure 5: Modeling a single attention block of GPT-2 for the prompt: “The capital of Japan is the city of”. The pop-up text windows are (from top to bottom): One of the memory values, whose source is the input token “Japan” and whose projection is highly correlated with the output of the model, “Tokyo” (1). The residual stream and the labels of its connected nodes (2). The input to the attention block after normalization, which its most probable token is “London” (3). One of the most activated neurons of  $W_O$  that has a negative coefficient. Its projection is highly unaligned with the model’s output, which the negative coefficient suppresses (4). At the block’s input, the chance for “Tokyo” is  $< 1\%$ , but at its output it is 25% (purple pop-up window (2)), i.e., this attention block prompts the meaning of “Tokyo”. The two biggest heads are “Yamato” (with Japanese concepts) and “cities”, which together create the output “Tokyo”.

### 3.4 Interim Summary

The analysis pictures a clear information flow, from a semantic perspective, in the attention block: [1] the block’s input creates a distribution on the previous keys resulting in a set of attention scores for each head (subsection 2.2), [2] which trigger the memory values created by previous tokens, where only the ones with the highest attention scores capture the head semantics (subsection 3.3). [3] The heads are concatenated into one vector, promoting the semantics of only a few heads (subsection 3.2) after they are projected to the vocabulary through  $W_O$  (subsection 3.1). An example of this procedure is shown for the prompt “The capital of Japan is the city of”, with the expected completion “Tokyo”, in Figure 1 for the flow in a full block and in Figure 5 for the flow in the attention sub-block. An input token like “Japan” might create a memory value with the meaning of Japanese concepts, like “Yamato” and “Samurai”. This memory value can capture its head meaning. Another head might have the meaning of the token “cities”, and together the output of the attention could be “Tokyo”.

## 4 Modeling the Information Flow as a Flow-Graph

As in most neural networks, information processing in an autoregressive LM can be viewed as a flow graph. The input is a single sentence (a sequence

of tokens), the final output is the probability of the next word, with intermediate nodes and edges. Geva et al. (2022b, 2021) focused on information flow in and across the MLP blocks, while our analysis in section 3 focused on the information flow in the attention block. In this section, we describe how to construct a readable and succinct graph for the full network, down to the level of individual neurons. Our graph is built on collected HS from a single forward pass: it uses single and small sets of HSs as nodes, while edges are the interactions between nodes during the forward pass.

One option for constructing a flow graph is to follow the network’s full computation graph. Common tools do this at the scale of matrices (Roeder, 2017), coarser than the neuronal scale we seek. They usually produce huge, almost unreadable, graphs that lack information on which values are passed between matrices and their effect. Similarly, if we were to connect all possible nodes (neurons and HSs) and edges (vector multiplications and summation), the graph would be unreadable, as there are thousands of neurons in each layer. Moreover, our analysis in section 3 shows that many components are redundant and do not affect the model’s intermediate processing. We therefore prune the graph to retain only the most relevant parts: by assigning scores to the edges at each computation step, like ranking the attention scores for

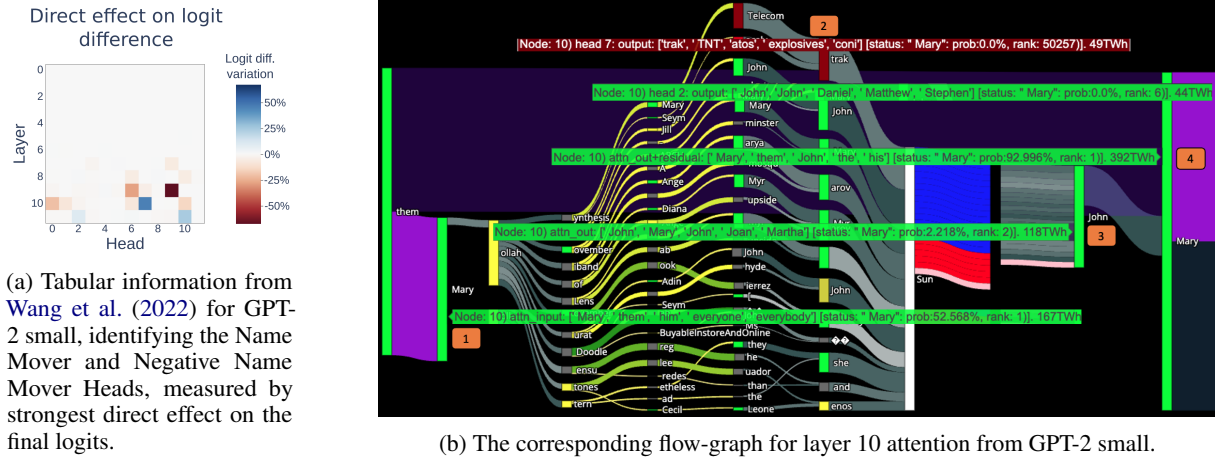


Figure 6: While 6a shows quantitative results, the graph model in Figure 6b shows qualitative information that is otherwise difficult to notice: The attention’s LN is the first place in the model where the attention input’s most probable token is “Mary” (1). The Negative Name Mover Head from layer 10, represented by the blue cell in the table’s 10-th row, is visualized in the graph with a red pop-up showing it assigns the token “Mary” its lowest possible ranking, meaning its role is to reduce the probability of this token (2). The output of the attention block is the token “John” but its second most probable output is “Mary” with around 2% chance (3). However, when added to the residual, together they predict almost 93% chance for “Mary” (4).

the edges connected to each memory value, or the activation score for neurons in MLPs, we present only the edges with the highest scores at each level. Nodes without any remaining edge are removed. The goal is to present only the main components that operate at each block. See subsection A.4 for details.

To present the semantic information flow, we assign each node with its most probable projected token and the ranking it gives to the model’s final prediction, according to the logit lens. Each node is colored based on its ranking, thereby emphasizing the correlation between the node’s meaning and the final prediction. Additionally, we utilize the width of the edges to reflect the scores used for pruning.

Figures 1 and 5 show static examples on one sentence, the first for a single transformer block’s graph and the second with an annotated explanation on the attention sub-blocks’s sub-graph.<sup>6</sup>

## 5 Example of Use and Immediate Discoveries

The flow-graph model is especially beneficial for qualitative examinations of LMs to enhance research and make new discoveries. In this section, we demonstrate this with several case studies.

### 5.1 Indirect Object Identification

Recently, Wang et al. (2022) tried to reverse-engineer GPT-2 small’s computation in indirect object identification (IOI). By processing prompts like “When Mary and John went to the store, John gave a drink to”, which GPT-2 small completes with “Mary”, they identified the roles of each attention head in the process using methods like changing the weights of the model to see how they affect its output. One of their main discoveries was attention heads they called Name Mover Heads and Negative Name Mover Heads, due to their part in copying the names of the indirect object (IO, “Mary”) or reducing its final score.

We ran the same prompt with the same LM and examined the flow-graph it produced. The flow graph (Figure 6b) is highly correlated to Wang et al.’s results (Figure 6a). While they provide a table detailing the impact of each attention head on the final prediction, our graph shows this by indicating which token each head promotes. For instance, heads that project the token “Mary” among their most probable tokens are the Name Mover Heads, while Negative Name Mover heads introduce the negative meaning of “Mary” (evident by the low probability of “Mary” in their projection, highlighted in red). Not only does our model present the same information as the paper’s table, which was produced using more complex techniques, but our modeling also allows us to observe how the

<sup>6</sup>Dynamic examples can be found (or generated) at <https://github.com/shacharKZ/Visualizing-the-Information-Flow-of-GPT>.

attention mechanism scores each previous token and recalls their memory values. For example, we observe that the Negative Name Mover in layer 10 obtains its semantics from the memory value produced by the input token “Mary”.

We do not claim that our model can replace the empirical results of Wang et al. (2022), but it could help speed up similar research processes due to the ability to spot qualitative information in an intuitive way. Also, the alignment between the two studies affirms the validity of our approach for a semantic analysis of information flow of GPTs.

## 5.2 Layer Norm as Sub-Block Filter

Layer norm (LN) is commonly applied to sub-blocks for numerical stability (Ba et al., 2016) and is not associated with the generation components, despite having learnable weights. We investigate the role of LN, focusing on the first LN inside a GPT-2 transformer block,  $ln_1$ , and apply the logit lens before and after it. We use the data from section 3 and, as a control group, random vectors. Figure 7 shows change in logit lens probability of all tokens after applying LN. The tokens whose probability decreases the most are function words like “the”, “a” or “not”, which are also tokens with high mean probability across our generations (although they are not the final prediction in the sampled generations). Conversely, tokens that gain most probability from LN are content words like “Microsoft” or “subsidiaries”. See more examples and analyses of the pre-MLP LN,  $ln_2$ , in Appendix D. These results suggest that the model uses LN to introduce new tokens into the top tokens that it compares at each block.

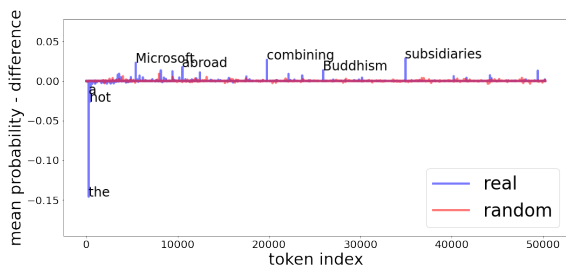


Figure 7: Differences in token probabilities before and after LN  $ln_1$  from layer 15 of GPT-2 medium. The horizontal axis is the index of all the tokens in GPT-2 and the vertical shows if the token lost or gained probability from the process (negative or positive value). We annotate the tokens that are most affected.

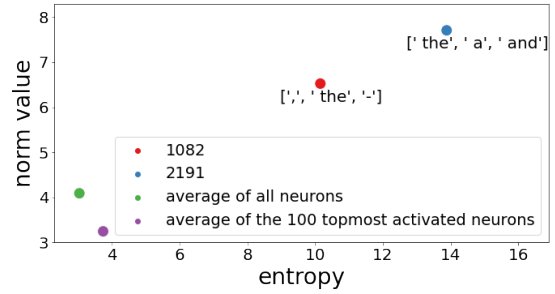


Figure 8: Entropy and norm of “regularization neurons” from the second MLP matrix of layer 19 compared to the matrix average and the 100 most activated neurons across 100 prompts from CounterFact.

## 5.3 Regularization Neurons

While browsing through many examples with our flow graph model, we observed some neurons that are always activated in the MLP second matrix,  $FF_2$ . We quantitatively verified this using data from section 3 and found that each of the last layers (18—23) has at least one neuron that is among the 100 most activated neurons more than 85% of the time (that is, at the top 98% most activated neurons out of 4096 neurons in a given layer). At least one of these neurons in each layer results in function words when projected with the logit lens, which are invalid generations in our setup. We further observe that these neurons have exceptionally high norms, but higher-entropy token distributions (closer to uniform), when projected via the logit lens (Figure 8). This suggests that these neurons do not dramatically change the probabilities of the final predictions.

By plotting these neurons’ weights, we find a few outlier weights with exceptionally large values (Figure 9). Since these neurons are highly activated, the outlier weights contribute to the phenomenon of outlier or rogue dimensions in the following HS, described in previous work (Puccetti et al., 2022; Timkey and van Schijndel, 2021; Kovaleva et al., 2021). This line of work also shows that ignoring those dimensions can improve similarity measures between embedded representations, while ignoring them during the computation of the model causes a significant drop in performance.

Our analysis adds a semantic perspective to the discussion on rogue dimensions: since these neurons’ projections represent “general” notions (not about a specific topic, like capitals or sports) and since they have high entropy, they might play a role

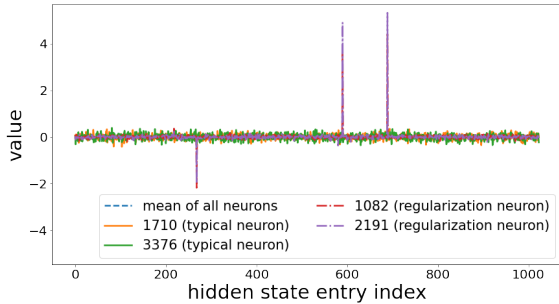


Figure 9: Plotting the value in each entry in the regularization neurons at layer 19, comparing the mean neuron and presenting two randomly sampled neurons that represent typical neurons. Those high magnitudes of the 3 entries in the regularization neurons help in the creation of the rogue dimensions phenomena.

of regularization or a sort of bias that is added as a constant to the residual stream. Finally, to reflect such cases, we paint all the accumulation edges in our flow-graph (where vectors are summed up) in grey, with darker shades expressing lower entropy.

## 6 Related work

Derived from the original logit lens (nostalgebraist, 2020), several studies analyze the role of each component in LMs using token projection (Geva et al., 2022b; Dar et al., 2022). In the last few months, new studies suggest trainable transformation for projecting HS (Din et al., 2023; Belrose et al., 2023), promising to better project neurons in the earlier layers of LMs (which currently seems to have less alignment with the final output than later ones).

Other work took a more mechanistic approach in identifying the role of different weights, mostly by removing weights or changing either weights or activations, and examining how the final prediction of the altered model is affected (Wang et al., 2022; Meng et al., 2022, 2023; Dai et al., 2022).

There has been much work analyzing the attention mechanism from various perspectives, like trying to assign linguistic meaning to attention scores or questioning their role as explanations. See Rogers et al. (2020) for an overview.

In the field of visualization tools for LM, Geva et al. (2022a) visualized the logit lens projection of the HSs between blocks and on the MLP weights. Other tools that focused on the attention described the connection between input tokens, (Hoover et al., 2020; Vig and Belinkov, 2019) but did not explore

the internals of the attention module. There are general tools for visualizing deep learning models, like Roeder (2017), but they only describe the flow of information between matrices, not between neurons. Strobelt et al. (2018a,b) visualize hidden states and attention in recurrent neural network models, allowing for interaction and counterfactual exploration.

## 7 Conclusion

In this work, we used token projection methods to trace the information flow in transformer-based LMs. We have analyzed in detail the computation in the attention module from the perspective of intermediate semantics the model processes, and assessed the interactions between the attention memory values and attention output, and their effect on the residual stream and final output.

Based on the insights resulting from our analysis, we created a new tool for visualizing this information flow in LMs. We conducted several case studies for the usability of our new tool, for instance revealing new insights about the role of the layer norm. We also confirmed the validity of our approach and showed how it can easily support other kinds of analyses.

Our tool and code will be made publicly available, in hope to support similar interpretations of various auto-regressive transformer models.

## Limitations

Our work is limited to English LMs, in particular different types of GPT models, and the quantitative analyses are done on a dataset of factual statements used in recent work. While our methodology is not specific to this setting, the insights might not generalize to other languages or datasets.

In this work we interpret HS and neurons using projection methods which are still being examined, as well the idea of semantic flow. The way we measure impact and distance between HS using  $I_k$  (the intersection between their top tokens) is not ideal since it might not convey the semantic connection of two different tokens with the same meaning. While it is possible to achieve more nuanced measurements with additional human resources (users) or semi-automatic techniques, there would be limitations in mapping a vast number of neurons and their interactions due to the enormous number of possible combinations. Therefore, we deliberately



chose not to employ human annotators in our research.

Our pruning approach is based on the assumption that the most activate neurons are the ones that determine the model’s final prediction. Although this claim is supported by our qualitative analysis, we cannot claim that the less activated neurons are not relevant for building the prediction. Since our flow-graph model does not show those less active neurons, it might give misleading conclusions.

Finally, our methods do not employ causal techniques, and future work may apply various interventions to verify our findings. Our tool tries to reflect what GPT “thinks”, but further investigation of its mechanism is needed before approaching a full understanding of this “black box”.

## Acknowledgements

This work was supported by the ISRAEL SCIENCE FOUNDATION (grant No. 448/20), Open Philanthropy, and an Azrieli Foundation Early Career Faculty Fellowship.

## Ethics Statement

Our goal is to improve the understanding of LMs. We dissect inner layers and intermediate results of GPT based on techniques that are already been used in other papers. The semantics behind some projections might appear offensive and we want to be clear that we have no intention of such.

Further work might use our new tool to try to identify components of the model that control a given idea or knowledge, and to edit it. We hope such a use case would be for better representing information and not for spreading any hate.

## References

Jimmy Lei Ba, Jamie Ryan Kiros, and Geoffrey E Hinton. 2016. Layer normalization. *stat*, 1050:21.

Nora Belrose, Zach Furman, Logan Smith, Danny Halawi, Igor Ostrovsky, Lev McKinney, Stella Biderman, and Jacob Steinhardt. 2023. Eliciting latent predictions from transformers with the tuned lens. *arXiv preprint arXiv:2303.08112*.

Damai Dai, Li Dong, Yaru Hao, Zhifang Sui, Baobao Chang, and Furu Wei. 2022. [Knowledge neurons in pretrained transformers](#). In *Proceedings of the 60th Annual Meeting of the Association for Computational Linguistics (Volume 1: Long Papers)*, pages 8493–8502, Dublin, Ireland. Association for Computational Linguistics.

Guy Dar, Mor Geva, Ankit Gupta, and Jonathan Berant. 2022. [Analyzing transformers in embedding space](#). *arXiv preprint arXiv:2209.02535*.

Alexander Yom Din, Taelin Karidi, Leshem Choshen, and Mor Geva. 2023. [Jump to conclusions: Short-cutting transformers with linear transformations](#). *arXiv preprint arXiv:2303.09435*.

N Elhage, N Nanda, C Olsson, T Henighan, N Joseph, B Mann, A Askell, Y Bai, A Chen, T Conerly, et al. 2021. [A mathematical framework for transformer circuits](#).

Mor Geva, Avi Caciularu, Guy Dar, Paul Roit, Shoval Sadde, Micah Shlain, Bar Tamir, and Yoav Goldberg. 2022a. [LM-debugger: An interactive tool for inspection and intervention in transformer-based language models](#). In *Proceedings of the The 2022 Conference on Empirical Methods in Natural Language Processing: System Demonstrations*, pages 12–21, Abu Dhabi, UAE. Association for Computational Linguistics.

Mor Geva, Avi Caciularu, Kevin Wang, and Yoav Goldberg. 2022b. [Transformer feed-forward layers build predictions by promoting concepts in the vocabulary space](#). In *Proceedings of the 2022 Conference on Empirical Methods in Natural Language Processing*, pages 30–45, Abu Dhabi, United Arab Emirates. Association for Computational Linguistics.

Mor Geva, Roei Schuster, Jonathan Berant, and Omer Levy. 2021. [Transformer feed-forward layers are key-value memories](#). In *Proceedings of the 2021 Conference on Empirical Methods in Natural Language Processing*, pages 5484–5495.

Adi Haviv, Ido Cohen, Jacob Gidron, Roei Schuster, Yoav Goldberg, and Mor Geva. 2023. [Understanding transformer memorization recall through idioms](#). In *Proceedings of the 17th Conference of the European Chapter of the Association for Computational Linguistics, EACL 2023, Dubrovnik, Croatia, May 2-6, 2023*, pages 248–264. Association for Computational Linguistics.

Benjamin Hoover, Hendrik Strobelt, and Sebastian Gehrmann. 2020. [exbert: A visual analysis tool to explore learned representations in transformer models](#). In *Proceedings of the 58th Annual Meeting of the Association for Computational Linguistics: System Demonstrations*, pages 187–196.

Plotly Technologies Inc. 2015. [Collaborative data science](#).

Olga Kovaleva, Saurabh Kulshreshtha, Anna Rogers, and Anna Rumshisky. 2021. [Bert busters: Outlier dimensions that disrupt transformers](#). In *Findings of the Association for Computational Linguistics: ACL-IJCNLP 2021*, pages 3392–3405.

Max Lamparth and Anka Reuel. 2023. [Analyzing and editing inner mechanisms of backdoored language models](#). *arXiv preprint arXiv:2302.12461*.

- Kevin Meng, David Bau, Alex Andonian, and Yonatan Belinkov. 2022. Locating and editing factual associations in GPT. *Advances in Neural Information Processing Systems*, 36.
- Kevin Meng, Arnab Sen Sharma, Alex Andonian, Yonatan Belinkov, and David Bau. 2023. Mass-editing memory in a transformer. *International Conference on Learning Representations*.
- nostalgebraist. 2020. [interpreting gpt: the logit lens](#).
- Giovanni Puccetti, Anna Rogers, Aleksandr Drozd, and Felice Dell’Orletta. 2022. Outliers dimensions that disrupt transformers are driven by frequency. *arXiv preprint arXiv:2205.11380*.
- Alec Radford, Jeff Wu, Rewon Child, David Luan, Dario Amodei, and Ilya Sutskever. 2019. Language models are unsupervised multitask learners. OpenAI blog.
- Lutz Roeder. 2017. [Netron, Visualizer for neural network, deep learning, and machine learning models](#).
- Anna Rogers, Olga Kovaleva, and Anna Rumshisky. 2020. A primer in BERTology: What we know about how BERT works. *Transactions of the Association for Computational Linguistics*, 8:842–866.
- H. Strobel, S. Gehrmann, H. Pfister, and A. M. Rush. 2018a. Lstmvis: A tool for visual analysis of hidden state dynamics in recurrent neural networks. *IEEE Transactions on Visualization and Computer Graphics*, 24(01):667–676.
- Hendrik Strobel, Sebastian Gehrmann, Michael Behrisch, Adam Perer, Hanspeter Pfister, and Alexander M Rush. 2018b. Seq2seq-vis: A visual debugging tool for sequence-to-sequence models. *IEEE transactions on visualization and computer graphics*, 25(1):353–363.
- William Timkey and Marten van Schijndel. 2021. All bark and no bite: Rogue dimensions in transformer language models obscure representational quality. In *Proceedings of the 2021 Conference on Empirical Methods in Natural Language Processing*, pages 4527–4546.
- Ashish Vaswani, Noam Shazeer, Niki Parmar, Jakob Uszkoreit, Llion Jones, Aidan N Gomez, Łukasz Kaiser, and Illia Polosukhin. 2017. Attention is all you need. *Advances in neural information processing systems*, 30.
- Jesse Vig and Yonatan Belinkov. 2019. Analyzing the structure of attention in a transformer language model. In *Proceedings of the 2019 ACL Workshop BlackboxNLP: Analyzing and Interpreting Neural Networks for NLP*, pages 63–76.
- Ben Wang and Aran Komatsuzaki. 2021. GPT-J-6B: A 6 Billion Parameter Autoregressive Language Model. <https://github.com/kingoflolz/mesh-transformer-jax>.
- Kevin Ro Wang, Alexandre Variengien, Arthur Conmy, Buck Shlegeris, and Jacob Steinhardt. 2022. Interpretability in the wild: a circuit for indirect object identification in gpt-2 small. In *NeurIPS ML Safety Workshop*.

## A Modeling GPTs as a Flow-Graph

This section presents a formal construction of GPTs as flow-graphs for single forward passes, followed by more implementation details. The information here supplements the brief description given in [subsection 2.2](#) and is brought here for completeness.

Like any graph, our graph is defined by a set of nodes (vertices) and edges (links). In our case, the graph follows a hierarchical structure, starting with the breakdown of the entire model into layers, followed by sub-blocks such as attention and MLP blocks, and eventually individual or small sets of neurons. A GPT model consisting of  $L$  transformer blocks denoted as  $B_l$  ( $0 \leq l < L$ ), where  $W_Q$ ,  $W_K$ ,  $W_V$ ,  $W_O$  represent the matrices for the attention block, and  $FF_1 = W_{FF1}$  and  $FF_2 = W_{FF2}$  represent the matrices for the MLP. We now walk through the forward computation in the model and explain how we construct the flow graph.

### A.1 The Attention Block as a Flow-Graph

1. The input to the  $l$ -th block for the  $t$ -th input,  $hs_t^l$ , passes through a LN, resulting in a normalized version of it. We create a node for the input vector and another node for the normalized vector, connecting them with an edge.
2. The normalized input is multiplied by  $W_Q$ ,  $W_K$ , and  $W_V$ , resulting in query, key, and value representations ( $q$ ,  $k$ ,  $v$ ). We create a single node to represent these three representations, as they are intermediate representations used by the model. We construct an edge between the normalized input and this node.
3. The last three representations ( $q$ ,  $k$ ,  $v$ ) are split into  $h$  heads ( $q_{jt}$ ,  $k_{jt}$ ,  $v_{jt}$  for  $0 \leq j < h$ ). Each head's query vector ( $q_{jt}$ ) is multiplied by all the previous key vectors ( $k_{ji}$  for  $1 \leq i \leq t$ ), calculating the attention probability for each of the previous token values. We create a node for each head's query vector and connect it with an edge to the overall query node created in the previous step. Additionally, we create a node for each key vector and connect it with an edge to its corresponding head's query vector.
4. Each memory value vector ( $v_{ji}$ , the memory value of the  $j$ -th head and the  $i$ -th input token), is summed up with a coefficient (the attention

score) into its corresponding head  $A_j$ . We create a node for each value vector and connect it with an edge to its corresponding key vector. Furthermore, we create a node for each summed-up head  $A_j$  and connect it to all of its memory value vectors. This establishes a direct path between each head's query  $q_{jt}$ , its keys  $k_{ji}$ , its values  $v_{ji}$ , and the head's final vector  $A_j$ . It is important to note that the calculation of attention scores is non-linear and preserves the relative ranking among memory values.

5. The  $h$  heads  $A_j$  are concatenated, resulting in a vector  $A_{concatenated}$  with the same size as the model's hidden state (embedding size). We create a node for  $A_{concatenated}$  and connect all the heads  $A_j$  to it.
6.  $A_{concatenated}$  is multiplied by  $W_O$  to produce the attention output  $Attn(hs_t^l)$ . We create a node for each entry in  $A_{concatenated}$  and each neuron in  $W_O$ , connecting them through edges representing the multiplication process. Additionally, we create a node for the output  $Attn(hs_t^l)$  and connect each neuron to it.
7. The attention output is then added to the residual stream of the model. We create a node for the sum of the attention block and the residual,  $hs_{attn+residual}$ , and connect it to  $Attn(hs_t^l)$ .
8. The attention block also contains a skip connection, The residual, from the input  $hs_t^l$  straight to the output  $hs_{attn+residual}$ , so we connect an edge between them.

### A.2 The Feed Forward Block as a Flow-Graph

This structure is mainly based on the theory of using two fully connected layers as keys and values, as described by [Geva et al. \(2021\)](#)

1. Similar to the attention block, the input to this block, denoted as  $\hat{hs}_t^l = hs_{attn+residual}$  (representing the intermediate value of the residual after the attention sub-block), passes through a layer norm, resulting in a normalized version of it. We create a node for the input vector and another node for the normalized vector, connecting them with an edge.
2. The normalized input is multiplied by  $W_{FF1}$ . For each neuron in the matrix, we create a

node and connect an edge from the normalized input to it (corresponding to the multiplication of each neuron separately).

3. The result of the previous multiplication is a vector of coefficients for the second MLP matrix,  $W_{FF2}$ . Consequently, we create a node for each neuron in  $W_{FF2}$  and connect an edge between each neuron and its corresponding neuron from  $W_{FF1}$ . It is important to note that the actual process includes a non-linear activation between the two matrices, which affects the magnitude of each coefficient but not its sign (positive or negative).
4. The neurons of  $W_{FF2}$  are multiplied by their coefficients and summed up into a single vector, which serves as the output of the MLP block, denoted as  $MLP(\hat{h}s_l^t)$ . We create a node for  $MLP(\hat{h}s_l^t)$  and connect all the neurons from  $W_{FF2}$  to it.
5. The output of the block is then added to the model’s residual stream. We create a node for the sum of the MLP block and the residual, denoted as  $h_{S_{MLP+residual}}$ , and connect it to  $MLP(\hat{h}s_l^t)$ .
6. Similarly to the attention block, the MLP block also includes a skip connection, directly connecting the input  $\hat{h}s_l^t$  to the output  $h_{S_{MLP+residual}}$ . Therefore, we connect an edge between them.

### A.3 Connecting The Graphs of Single Blocks Into One

In GPT-2 each transformer block contains an attention block followed by a MLP block. We define a graph for each transformer block by the concatenation of its attention graph and MLP graph, where the two graphs are connected by an edge between the attention’s  $h_{S_{attn+residual}}$  and the MLP’s  $\hat{h}s_l^t$ . The input to the new graph is the input of the original attention sub-graph, and its output is the output of the original MLP sub-graph.

To define the graph of the entire model we connect all its transformer blocks’ sub-graphs into one graph by connecting an edge between each block’s sub-graph output and the input of its following block’s sub-graph. The input to the new graph is the input of the first block and the output is the final block output.

### A.4 Scoring the Nodes and Edges

In order to emphasize some of the behaviors of the models, we define scoring functions for its nodes and edges.

**Scoring nodes according to projected token ranking and probability:** as we described, each node is created from a vector that we project to the vocabulary space, resulting in a probability score that defines the ranking of all the model’s tokens. Given a specific token  $w$  and a single vector  $v$  we define its neuronal ranking and probability,  $v_{rank}(w)$  and  $v_{prob}(w)$ , as the index and probability of token  $w$  in the projected vector of  $v$ .

**Scoring edges according to activation value and norm:** There are two types of edges: edges that represent the multiplication of neurons with coefficients (representing neuron activation) and edges that represent summation (as part of matrix multiplication). Edges that represent multiplication with coefficients are scored by the coefficient. We also include in this case the attention scores, which are used as coefficients for the memory values. Edges that represent summation are scored by the norm of the vector which they represent. This scoring aims to reflect the relative involvement of each of the weights, since previous work found that neurons with higher activation or norm have a stronger impact on the model behavior (Geva et al., 2022b).

### A.5 Modeling a Single GPT Inference as a Flow-Graph

Given a prompt  $x_1, \dots, x_t$  we pass it through a GPT model and collect every HS (input and output of each matrix multiplication). Then we create the flow-graph as described above, where the input and HS are according to the last input token  $x_t$  and the attention memory (previous keys and values) correspond to all the input tokens. This process results in a huge graph with many thousands of nodes even for small models like GPT-2 small (Radford et al., 2019), which in this sense can only be examined as tabular data, similar to previous work. Since our goal is to emphasize the flow of data, we reduced the number of nodes according to our discoveries and the assumption that neurons in the MLP blocks with relatively low activation have a small effect on the model output (Geva et al., 2022b). We also note that with a simple adjustment our model can show any number of neurons or show only chosen ones.



The reduced graph is defined as follows:

- In the attention sub-graph, we chose to present all the nodes of the heads' query and output,  $q_{jt}$ ,  $A_j$ , but to present only the memory keys and values,  $k_{ji}$ ,  $v_{ji}$ , that received the highest attention score, in light of the results from Section 3.1. We also decided to present only the top most activated neurons of  $W_O$ , according to the largest entries (by absolute value) from its coefficients HS,  $A_{concated}$ .
- In the MLP sub-graph we decided to show only the nodes of the most activated neurons. The activation is determined by the highest absolute values in the HS between the two matrices after the nonlinearity activation. That is, we examine the input to the second MLP matrix  $W_{FF2}$  and present only the nodes that are connected to its highest and lowest entries.
- We make it possible to create a graph from only part of consecutive transformer blocks, allowing us to examine only a few blocks at a time.

The above simplifications help construct a scalable graph that humans can easily examine.

## A.6 Implementation Details and how to Read the Graph

We use the Python package Plotly-Express (Inc., 2015) to create a plot of the model. We provide all the source code we created to model the GPT-2 family models (small, medium, large and XL) and GPT-J (Wang and Komatsuzaki, 2021), with the latter code serving as a guided example with instructions designed to facilitate the adaptation of our flow-graph model to other GPT models.

Using our tool is straightforward and only requires running our code. The flow-graph plot can be presented in your software environment or saved as an HTML file to view via a browser. Personal computers and environments like Google Colab are sufficient for modeling LMs like GPT-2 medium, even without GPU. Plotly-Express allows us to inspect the created graphs interactively, like seeing additional information when hovering over the nodes and edges, or to filter some of them by the "Select" options on the top right of the generated plots.<sup>7</sup>

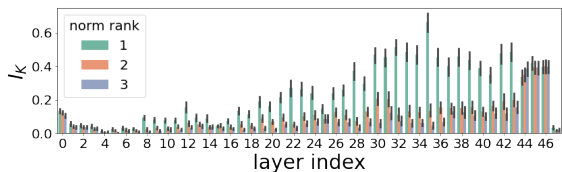
<sup>7</sup>More existing examples and the code for creating new ones can be found at <https://github.com/shacharKZ/Visualizing-the-Information-Flow-of-GPT>

The basics on how to read and use the flow-graph plots are:

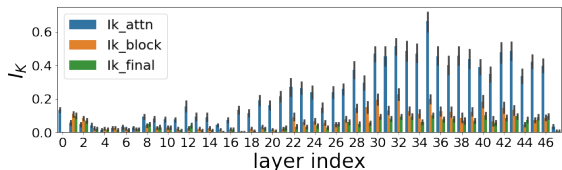
- The flow is presented from left to right (matrices that operate earlier during the forward pass will be to the left of later ones). When plotting a single block we can identify the attention sub-block (the first from the left) and the MLP sub-block as they are connected by a wide node and by separate and parallel wide edges representing the residual (each with a slightly different color). When plotting more than one block we can identify the different blocks by the repetitive structure of each.
- Each node is labeled with its most probable projected token. When hovering over a node, we can see from which layer and from which HS or matrix it was taken (the first number and the follow-up text in the pop-up text window. For example: "10) attn-input" suggest this node is the input of the attention sub-block in layer 10). The other information when hovering over each node is its top most probable tokens (a list of tokens) and "status", suggesting its relation with another token, "target", chosen by the user (if given); in particular, its probability and ranking for that token.
- In the attention score calculation we can locate which previous key and value were created by which of the input tokens, since they have the same indexes in the attention memory implementation of GPT-2. We present this information by hovering over the nodes in the attention sub-graph.
- Hovering over an edge presents which nodes it connects to along with information about what it represents, for example: if it is an edge between an attention query and key, it will represent the attention score between them. If the edge represents a summation of one HS into another, the information on the edge will be the norm of the summed HS.
- A user invoking the code can choose the model, the prompt, which layers to present, and a "target" token (which we recommend to be the actual output of the model for the given prompt).

## B Model Selection

As mentioned, we used GPT-2 medium (355M parameters) as our main case study due to its availability, wide use in previous research, the ability to run it even with limited resources, and the core assumption that characteristics we see with it are also relevant to bigger models. To validate ourselves, we also ran parts of our quantitative analysis with GPT-2 XL (1.5B parameters) with the same setup as we had with the medium model, and observed the same behavior; for example, see Figure 10. For these reasons we believe our analysis and modeling are applicable to general GPT-based models and not only to a specific model.



(a) Mean  $I_{k=50}$  for only the 3 heads with the largest norm, comparing to attention block output.



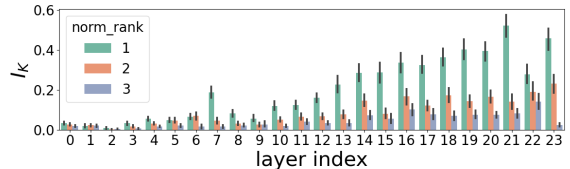
(b) Mean  $I_{k=50}$  for only the top-norm head, comparing to attention block output, layer output, and the model’s final output.

Figure 10: Projecting attention heads of GPT-2 xl, with the same setups as in Figure 3, shows that the patterns we saw with GPT-2 medium are similar to the ones we see with a bigger model.

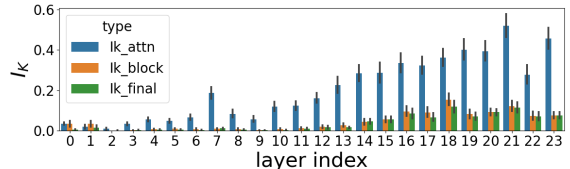
## C Additional Quantitative Analysis of Information Flow Inside the Attention Blocks

### C.1 Additional Setup Information

We provide here additional information on our setup and data selection. The choice of using CounterFact is based on its previous usage in studies on identifying where information is stored in models (Meng et al., 2022, 2023). However, it has the issue that GPT-2 does not succeed in answering most of its prompts correctly (only approximately 8% for GPT-2 medium and 14% for GPT-2 xl), and in many cases, the model’s predictions consist primarily of function words (like the token “the”).



(a) Mean  $I_{k=50}$  for only the 3 heads with the largest norm, comparing to attention block output.



(b) Mean  $I_{k=50}$  for only the top-norm head.

Figure 11: Projecting attention heads for prompts from CounterFact, without filtering prompts the model does not answer correctly. These show almost the same results as with the main setup in Figure 3, suggesting the mechanism behind the model’s attention works the same for correctly recalling factual knowledge and when predicting tokens of function words.

To avoid editing prompts or analyzing uninteresting cases, we decided to use only prompts that the model answers correctly. A plausible question is whether the model acts differently when it predicts the right answer compared to the general case, without filtering by answer correctness. To examine this we ran our analysis twice, once with only prompts the model knows to answer (like we explain in Section 3) and another time with random prompts from CounterFact. It turns out that the attention mechanism works the same way in both setups, resulting in almost the same graphs (Figure 11), which suggests that the behavior we saw is not restricted to recalling factual knowledge.

The only main difference we notice is the probability score the models give to their final prediction along the forward pass: when the model correctly predicts the CounterFact prompt (meaning it recalls a subject) it starts to assign the prediction high probabilities around its middle layers. However, when the model predicts incorrectly (and mostly predicts a function word), it assigns moderate probabilities starting from the earlier layers (Figure 12). This might suggest for later works to examine if factual knowledge, which is less common than function words in general text, is located in deeper layers as opposed to non-subject tokens.

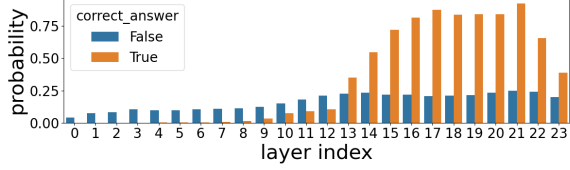


Figure 12: The probability GPT-2 medium assigns to its final predictions' tokens for the projection of the HS between blocks, colored by whether the model returns the true answer or not.

## C.2 Additional Results

We add more graphs to the analysis in Section 3 that help explain our claims in the conclusion of that part. All results are taken from the same experiment we used in that section. Notice that according to the following analysis the model exhibits distinct behavior during its initial 4–6 layers (out of 24) compare to the subsequent layers, as indicated by the low  $I_k$  scores for the first layers (Figures 13, 14), a behavior that was noted in previous work (Geva et al., 2022b; Haviv et al., 2023; Dar et al., 2022) and is yet to be fully understood.

Figure 13 illustrates the relationship between the attention output and the residual. It showcases the incremental changes that occur in the residual as a result of the attention updates to it. Similar to how the MLP promotes conceptual understanding within the vocabulary (Geva et al., 2022b), the attention layers accomplish a similar effect from the perspective of the residual. Furthermore, the figure reveals the high similarity in semantics between each attention sub-block and its preceding attention sub-block.

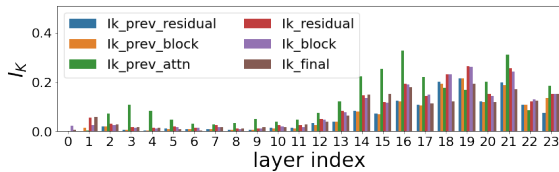


Figure 13: Comparing  $I_{k=50}$  of attention output with its current and previous residual (just after it is updated with the attention output) and the block output (note that the input of the attention sub-block is its previous block output). The intersection between the attention output is considered high, which means that the attention sub-blocks have overlapping semantics between different layers.

Figure 15 demonstrates that the information flow we saw from the memory values to the heads output

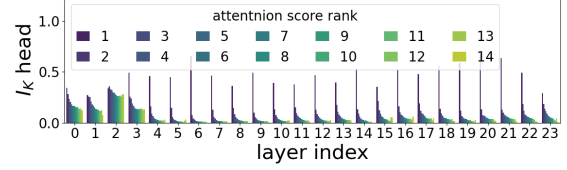


Figure 14: Comparing  $I_{k=50}$  of memory values with the output of their heads, according to the memory value norm rank compared to other values in the same head (the complete analysis behind Figure 4). This example claims that the semantics of each head is determined by its top memory value since only the top 1–3 memory values have some semantic intersection with their heads (starting from the 4-th layer) and the rest of the heads have almost no intersection (the number 14 suggest that the longest input we used for this experiment was 14 tokens).

is a behavior that applies to all heads.

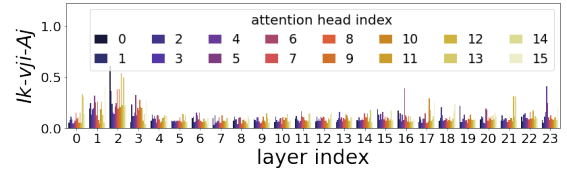


Figure 15: Comparing  $I_{k=50}$  of memory values with the output of their heads, according to head indices. This shows that there are no particular heads that are more dominant than others (after the first few layers).

Figure 16 demonstrates the alignment in projection correlation between each input token and its corresponding memory values. For every memory value  $v_{ji}$ , we examine the probability of its input token (the  $i$ -th input token) after applying a logit lens to  $v_{ji}$ . Our underlying assumption is that if the generated values share common semantics, then the probability of the input token should be higher than random (which is nearly 0). The results substantiate this assumption, revealing higher scores in the subsequent layers.

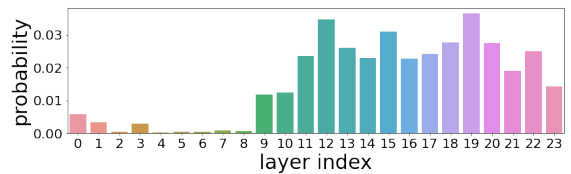


Figure 16: The probability of input token in the vectors of memory values they generated.

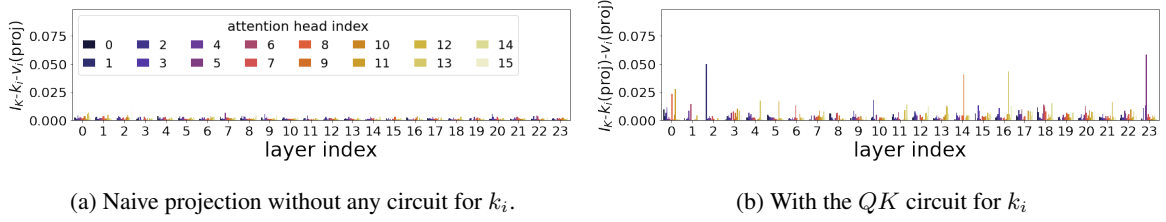


Figure 17: Comparing  $I_{k=50}$  token projection alignment between the head outputs of  $W_K$  and  $W_V$  ( $k_i$  and  $v_i$ ), with and without the  $QK$  circuit for  $W_K$  ( $v_i$  is projected with  $W_O$  and can be seen as the output of the  $OV$  circuit).

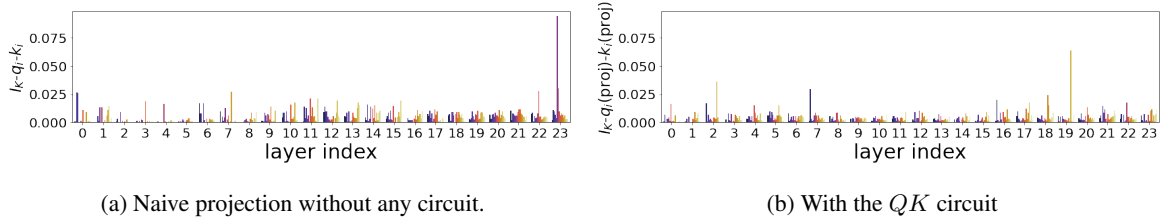


Figure 18: Comparing  $I_{k=50}$  token projection alignment between the head outputs of  $W_Q$  and  $W_K$  ( $q_i$  and  $k_i$ ), with and without the  $QK$  circuit. The mean intersection for two random sampling of 50 items (without duplication) from a set the size of GPT-2 vocabulary (50257) is around 0.05 matches, which equals to  $I_{k=50}$  of 0.001. However, when we apply the logit lens to two random vectors, it is observed that due to certain biases in the decoding process, the average  $I_{k=50}$  value is 0.002.

### C.3 Are All HS Interpretable? Examining the $QK$ Circuit

Similar to our analysis of the attention matrices  $W_V$ ,  $W_O$  (section 3), we try to find alignment between  $W_Q$ ,  $W_K$  outputs and other HS of the model. The work of Dar et al. (2022), who first projected the matrices  $W_Q$ ,  $W_K$ , emphasizes the importance of projecting the interaction between the two using the  $QK$  circuit, meaning by projecting the matrix  $W_{QK} = W_Q \cdot W_K$ . Using the data from section 3, we collected dynamic HS that these matrices generate,  $q_i$  and  $k_i$  (attention queries and keys), to examine their alignment between each other and between the memory value  $v_i$  they promote (each  $k_i$  leads to a single  $v_i$ , noting we already saw the latter is aligned with the attention’s and model’s outputs section 3). We project  $q_i$  and  $k_i$  using two methods: once with the naive logit lens ( $LL$ ) and once using the  $QK$  circuit, by first multiplying  $q_i$  with  $W_K$  ( $LL(q_i \cdot W_K)$ ) and  $k_i$  with  $W_Q$  ( $LL(W_Q \cdot k_i)$ ). Our hypothesis was that we will see some overlap between the top tokens of  $q_i$ ,  $k_i$  and  $v_i$ ; however, the results in Figures 17, 18 show almost no correlations using both methods, in contrast to the results we saw with  $W_V$  and  $W_O$  (subsection 3.1).

We believe there are two options for the low scores we see. The first option is that  $W_Q$  and  $W_K$  deliberately promote different tokens, with no alignment between  $W_Q$ ,  $W_K$ ,  $W_V$ . The idea

behind that is to check the associations between different ideas (for example, an unclear association can be a head’s keys  $k_i$  with meanings about sports but with values  $v_i$  about the weather). Another option is that the output of  $W_Q$ ,  $W_K$  operates in a different embedding space, which is different than the rest of the model, explaining why logit lens would not work on it. A support for this idea can be the fact that the output of these matrices is not directly summed up with the residual, but is only used for computing of the attention scores (that are used as coefficients for  $v_i$ , which are summed into the residual).

In our flow graph model, the user can choose to merge  $q_i$ ,  $k_i$  nodes into one with  $v_i$ , making them less visible. However, we decided to display them by default and to project them with the  $QK$  circuit, since during our short qualitative examination we noticed examples that suggest that the first option we introduced might be true. In Figure 6b we can see that the projection of the key with the highest attention score behind the Negative Name Mover Head holds the meaning of “Mary”. In this case, we can imagine that the model implements a kind of if statement, saying that if the input has really strong semantics of “Mary”, we should reduce a portion of it (maybe, to avoid high penalty when calculating the loss during training).



## D Layer Norm Uses as Sub-Block Filters

We present additional results about the role of LN in changing the probabilities of each sub-blocks’ input, including results for both LN layers in GPT-2. Tables 1 and 2 show the top tokens before and after  $ln_1$  for two different layers. Figure 19 gives a broader look at the effect of  $ln_1$ , detailing some examples across layers in Table 3. We repeat these analysis with  $ln_2$  in Figure 20 and Tables 4 and 5.

We include an example about the LN effect on the HS if the projection was done without the model’s final LN,  $ln_f$ , which is attached to the decoding matrix. Initially done to examine the effect of  $ln_1$  and  $ln_2$  without  $ln_f$  on projection, the results in Figure 21 and Table 6 highlight the importance of using  $ln_f$  as part of the logit lens projection, since the tokens we receive otherwise look out of the context of the text and tokens our model promotes in its generation.

before $ln_1$	after $ln_1$
English	English
the	Microsoft
Microsoft	abroad
North	subsidiaries
not	North
abroad	combining
a	downtown
London	Redmond
India	origin
origin	London

Table 1: The top tokens before and after  $ln_1$  at layer 15, according to the mean HS collected in section 3. We can see how the LN filters all the function words from the 10 most probable tokens while introducing instead new tokens like “Redmond” and “downtown”.

before $ln_1$	after $ln_1$
the	abroad
not	Microsoft
abroad	subsidiaries
a	combining
origin	English
Microsoft	origin
T	not
Europe	Europe
U	photographer
C	the

Table 2: The top tokens before and after  $ln_1$  at layer 13.

$ln_1$ 5	$ln_1$ 11	$ln_1$ 17	$ln_1$ 23
the	the	the	the
using	not	North	a
not	a	Google	English
this	T	a	India
within	C	South	Russian
in	U	company	German
,	in	now	North
and	,	Germany	South
:	which	not	"
outside	N	still	K

Table 3: Tokens that lose the most probability after  $ln_1$ , as collected from the experiment in section 3. Earlier layers’ LNs demote more tokens representing prepositions than later layers.

before $ln_2$	after $ln_2$
the	English
not	Microsoft
English	not
abroad	abroad
Microsoft	subsidiaries
a	origin
origin	combining
T	the
U	photographer
photographer	renowned

Table 4: The top tokens before and after  $ln_2$  at layer 13.

$ln_2$ 5	$ln_2$ 11	$ln_2$ 17	$ln_2$ 23
the	the	the	the
in	a	Google	a
a	T	French	German
using	U	Boeing	North
,	in	company	South
and	C	a	K
:	,	London	"
now	:	not	N
this	and	sports	Kaw
at	at	hockey	Boeing

Table 5: Tokens that lose the most probability after  $ln_2$ , similarly to Table 3.

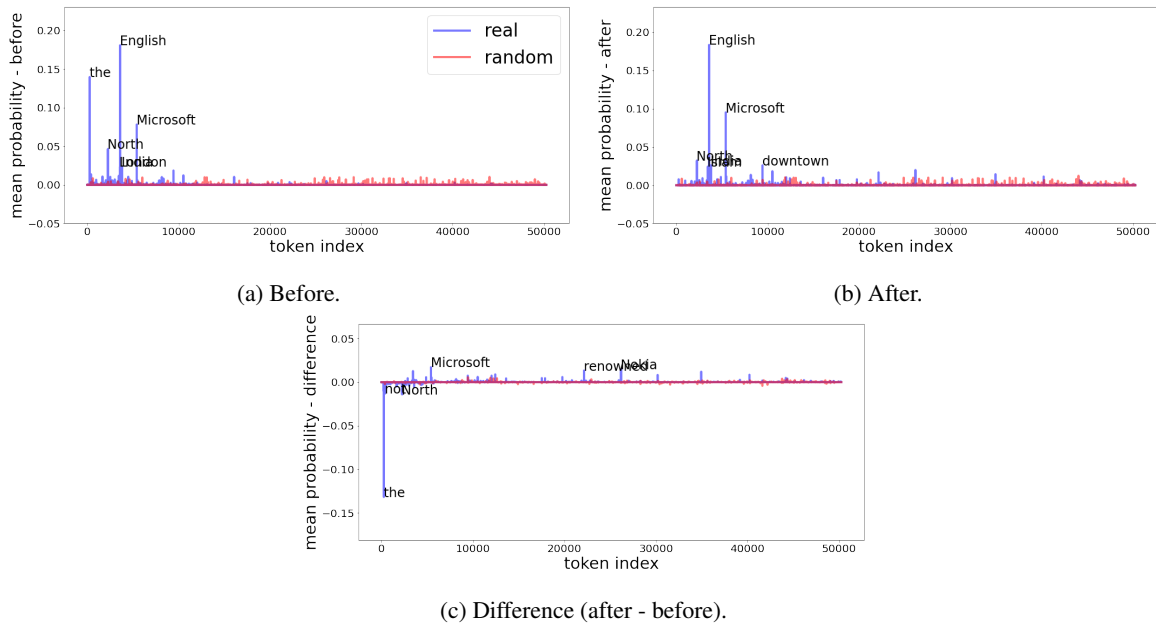


Figure 19: The probability of all the tokens in GPT-2 before and after the first LN,  $ln_1$ , in layer 16, including annotation for the largest-magnitude tokens. We see the difference in the distributions of tokens between randomly generated vectors and the ones we sample from CounterFact, which we find reasonable when answering factual questions. Especially if the questions are about a finite number of domains, the network promotes tokens not in a uniform way (like the random vectors does). Although tokens like “Microsoft” and “The” have a high probability before the LN, while the first gained more probability during the process the second actually loses, suggesting this is not a naive reduction to the probable tokens at each HS.

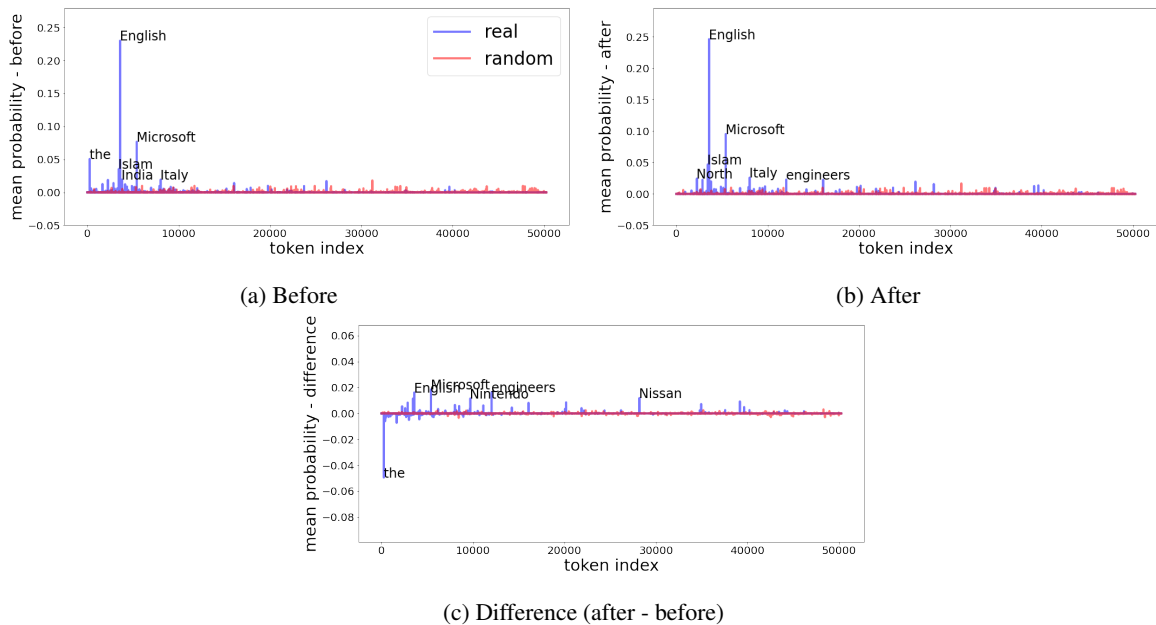


Figure 20: The effect of  $ln_2$  at layer 16 on tokens’ probabilities. We can see similar highly probable tokens as in Figure 19, since the only difference between the inputs of  $ln_1$  and  $ln_2$ , which is the residual stream, is the attention output of that layer (which is known to be gradual and does not steer the probability distribution dramatically Figure 12, 13).

$ln_1$ 5	$ln_1$ 11	$ln_1$ 17	$ln_1$ 23
Zen	not	the	the
imperialist	the	English	,
Sponsor	Europe	a	"
abroad	C	"	-
mum	abroad	football	ゼウス
utilizing	T	and	externalToEVAOnly
UNCLASSIFIED	pure	Toronto	sqor
conjunction	English	sports	quickShipAvailable
tied	ized	first	龍契士
nineteen	Washington	-	ÃÃÃÃÃÃÃÃ

Table 6: Top tokens that lost probability after applying  $ln_1$  when projection is done without  $ln_f$ .

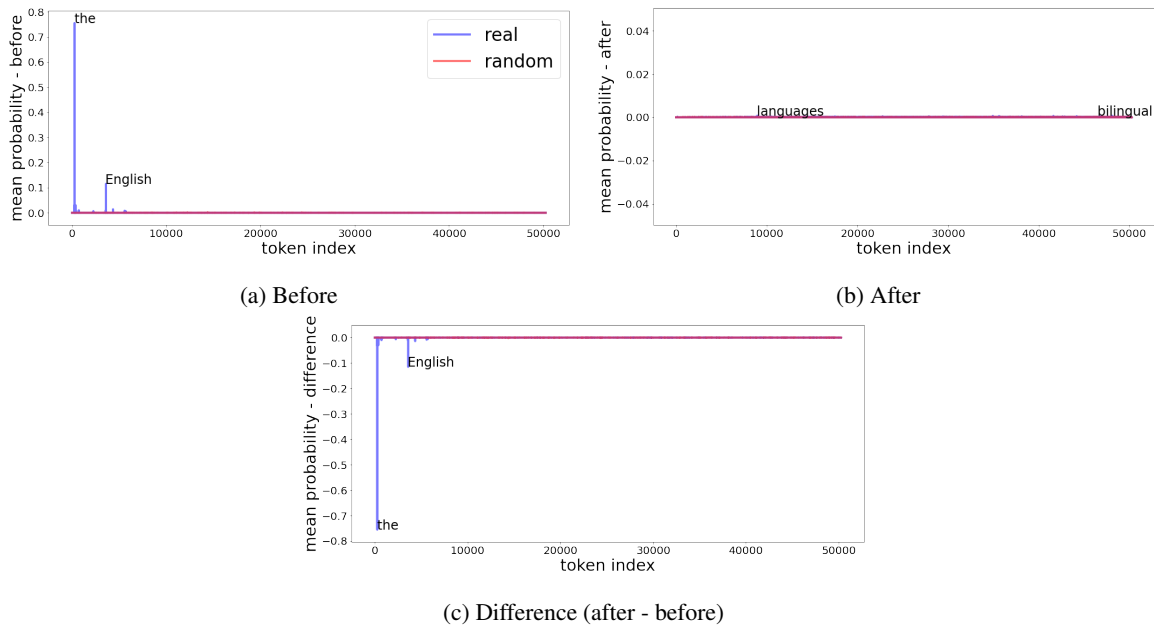


Figure 21: The affect of  $ln_1$  at layer 16 on tokens' probabilities (similar to Figure 19), but when the projection is done without  $ln_f$ .